

5) The feasibility of a focal point appears to be only realistic when adipose tissue (breast cancer) is irradiated. Because of the large lateral dimensions of the applicators, only two or three radiators can be grouped with reasonable size. As already mentioned, the applicator size is approximately 5 cm at 2450 MHz. At 915 MHz and irradiating fat, the applicator diameter would be about 13 cm (corresponding to a penetration depth of 14 cm [1]). Making the applicator dimensions smaller than these values would result in a rapid decrease of penetration depth, thus losing the benefits of the lower frequency. The same remarks are valid for the frequency of 433 MHz, where the required applicator diameter would be 30 cm.

These results have been checked with fair accuracy by experiments using muscle phantom and pork adipose tissue. Deviations from the above statements are likely to occur for the *in vivo* situation, because of the presence of the dynamics of a living system, like, for instance, blood flow. However, it is assumed that this could only affect the effective penetration depth of the used frequency by surface cooling effects of the blood stream and heat convection, and heat conduction to the interior. The principal features of the various systems should remain unchanged.

## REFERENCES

- [1] A. W. Guy, J. F. Lehmann, and J. B. Stonebridge "Therapeutic applications of electromagnetic power," *Proc. IEEE*, vol. 62, pp. 53-75, 1974.
- [2] J. W. Hand and G. ter Haar, "Heating techniques in hyperthermia," *Brit. J. Radiol.*, vol. 54, pp. 443-466, 1981.
- [3] D. A. Cristensen and C. H. Durney, "Hyperthermia production for cancer therapy: A review of fundamentals and methods," *J. Microwave Power*, vol. 16, pp. 89-105, 1981.
- [4] G. Kantor, "Evaluation and survey of microwave and radio-frequency applicators," *J. Microwave Power*, vol. 16, pp. 135-150, 1981.
- [5] G. M. Samaras, A. Y. Cheung, and S. F. Weinmann, "Focussed microwave radiation therapy for deep tumors," in *Hyperthermia as an Antineoplastic Treatment Modality*, NASA Publ. 2051, 1978, pp. 67-68.
- [6] A. Y. Cheung, W. M. Golding, and G. M. Samaras, "Direct contact applicators for microwave hyperthermia," *J. Microwave Power*, vol. 16, pp. 151-159, 1981.
- [7] F. A. Gibbs, "Clinical evaluation of a microwave/radio-frequency system (BSD Corporation) for induction of local and regional hyperthermia," *J. Microwave Power*, vol. 16, pp. 185-192, 1981.
- [8] M. Melek and A. P. Anderson, "A thinned cylindrical array for focussed microwave hyperthermia," in *Proc. 11th European Microwave Conf.* (Amsterdam), pp. 427-432, 1981.
- [9] H. P. Schwan, "Survey of microwave absorption characteristics of body tissue," in *Proc. Tri-Serv. Conf. on Biological Effects of Microwave Energy*, NTIS Doc. AD 131477 and 220124, pp. 126-145, 1958.
- [10] M. A. Stuchly and S. S. Stuchly, "Dielectric properties of biological substances—Tabulated," *J. Microwave Power*, vol. 15, pp. 19-26, 1980.
- [11] J. L. Guerquin-Kern, L. Palas, M. Gautherie, C. Fournet-Fayas, E. Gimonet, A. Priou, and S. Samsel, "Etude comparative d'appliqueurs hyperfréquences (2450 MHz, 434 MHz) sur fantômes et sur pièces opératoire, en vue d'une utilisation thérapeutique de l'hyperthermie micro-onde en cancérologie," in *Proc. URSI Symp. (Electromagnetic Waves and Biology)* (Jouy-en-Josas), pp. 241-247, 1980.

## Field Theory of Planar Helix Traveling-Wave Tube

DEVI CHADHA, SHEEL ADITYA, MEMBER, IEEE, AND  
RAJENDRA K. ARORA, SENIOR MEMBER, IEEE

**Abstract**—A pair of unidirectionally conducting screens, conducting in different directions, constitute a planar helix. The planar helix is proposed as a slow-wave structure for application in a traveling-wave tube (TWT).

Manuscript received March 29, 1982; revised August 4, 1982.  
The authors are with the Department of Electrical Engineering, Indian Institute of Technology, Hauz Khas, New Delhi, 110016, India.

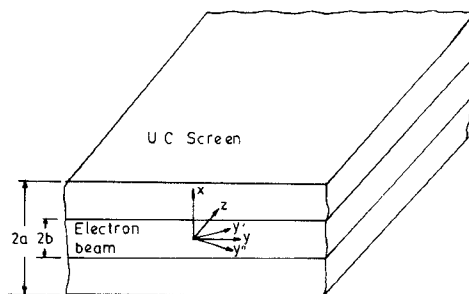


Fig. 1. The planar traveling-wave tube:  $z$ —direction of propagation;  $y'$  and  $y''$ —directions of conduction of top and bottom UC screens, respectively;  $\theta$ —helix angle.

Field theory is applied to analyze the behavior of the planar helix in the presence of a flat electron beam present between the two screens. Results indicate the presence of three modes, with one mode having a negative attenuation constant, as in the case of the usual helix-type TWT. Curves are shown for a typical proposed planar TWT. Also, the effect of beam current is indicated.

## I. INTRODUCTION

The analysis of a helix-type traveling-wave tube (TWT) has been carried out by Pierce [1], Chu and Jackson [2], and others [3], [4]. In a TWT, a slow-wave structure such as a helix or coupled cavity is used to slow down the electromagnetic wave to the velocity of the electron beam so that a strong interaction between the two can take place. A slow-wave structure in planar geometry, consisting of a pair of parallel unidirectionally conducting (UC) screens conducting in different directions and separated by some distance, has been studied by Arora [5], Aditya [6], and Aditya and Arora [7]. It appears that this planar slow-wave structure can be used in a TWT. In view of this, a planar helical TWT is analyzed in the present text. Field equations are derived and the modal solution of the problem is obtained. The variation of the complex propagation constants of different modes with beam voltage is studied.

## II. CONFIGURATION

The planar TWT considered here for analysis consists of a pair of UC screens (Fig. 1) separated by a distance  $2a$  in the  $x$ -direction. As shown, the top and the bottom screens conduct in directions  $y'$  and  $y''$  which, respectively, make angles  $\theta$  and  $-\theta$  with the  $y$ -axis. An electron beam of thickness  $2b$  is symmetrically located between the two screens. Both the screens and the beam are assumed to be of infinite extent in the  $y$ -direction. As pointed out in [5], limiting the structure in the transverse direction will not disturb the wave in regions remote from the ends, and results obtained here will be applicable to a structure several wavelengths wide. A practical structure can be terminated in the  $y$ -direction by closing the "helix" by conducting wires. The beam current density is constant over the cross section and has only a  $z$ -component. In practice, this assumption is very nearly realized by means of the focusing action of a strong dc magnetic field applied in the  $z$ -direction.

## III. WAVE EQUATIONS AND ELECTRON DYNAMICS

The boundary conditions require both TE and TM modes to be present. If the fields are assumed to be varying as  $\exp(j\omega t - \Gamma z)$ , and are constant in the  $y$ -direction, i.e.,  $\partial/\partial y \equiv 0$ , then the field equations can be written in the following form.

For the TE mode

$$\begin{aligned} \Gamma E_y + j\omega\mu_0 H_x &= 0 \\ \Gamma H_x + (\partial H_z / \partial x) + j\omega\epsilon_0 E_y &= 0 \\ \frac{\partial E_y}{\partial x} + j\omega\mu_0 H_z &= 0. \end{aligned} \quad (1)$$

For the TM mode

$$\begin{aligned} \Gamma H_y - j\omega\epsilon_0 E_x &= 0 \\ -\Gamma E_x - \frac{\partial E_z}{\partial x} + j\omega\mu_0 H_y &= 0 \\ \frac{\partial H_y}{\partial x} - j\omega\epsilon_0 E_z &= J_z \end{aligned} \quad (2)$$

where  $\Gamma = \alpha + j\beta$  is the propagation constant along the  $z$ -direction, and  $J_z$  is the  $z$ -component of the current density. It is seen from the field equations that the TE mode is unaffected by the presence of the beam and hence the wave equation for it remains unchanged and is given as

$$\frac{\partial^2 H_z}{\partial x^2} - u^2 H_z = 0 \quad (3)$$

where

$$u^2 = -\Gamma^2 - k_0^2$$

and

$$k_0^2 = \omega^2 \mu_0 \epsilon_0.$$

However, the TM mode is affected because of the presence of the  $z$ -component of current and the wave equation changes into

$$\frac{\partial^2 E_z}{\partial x^2} - u^2 E_z - \frac{u^2}{J\omega\epsilon_0} J_z = 0. \quad (4)$$

With the help of the continuity and force equations for the charges, the relationship between  $J_z$  and  $E_z$  can be obtained [1] as

$$J_z = - \left[ \frac{J\omega_p^2}{\omega} \frac{\beta_e^2 \epsilon_0}{(\beta_e + j\Gamma)^2} \right] E_z. \quad (5)$$

In (5),  $\omega_p^2 = \rho_0 e / m \epsilon_0$  and  $\beta_e = \omega / v_0$ , where  $\rho_0$  is the average charge density,  $e/m$  is the charge-to-mass ratio of the electron, and  $v_0$  is the average value of electron velocity. Thus using (5), the wave equation for the TM mode becomes

$$\frac{\partial^2 E_z}{\partial x^2} - p^2 E_z = 0 \quad (6)$$

where

$$p^2 = -(\Gamma^2 + k_0^2) \left[ 1 - \left( \frac{\omega p}{\omega} \right)^2 \left( \frac{\beta_e}{\beta_e + j\Gamma} \right)^2 \right]. \quad (7)$$

#### IV. BOUNDARY CONDITIONS AND CHARACTERISTIC EQUATION

Fig. 2 shows the structure in cross section. The symmetry about the plane  $x = 0$  suggests the general solution to be separable into two types of modes: 1) transverse-symmetric (even) and 2) transverse-antisymmetric (odd). In the former type, the transverse field components are symmetrical with respect to  $x$ , while the longitudinal components  $E_z$  and  $H_z$  are antisymmetrical. Similarly, in the latter type of modes, the opposite is true. Symmetry ensures that only one half of the structure need be considered in the analysis.

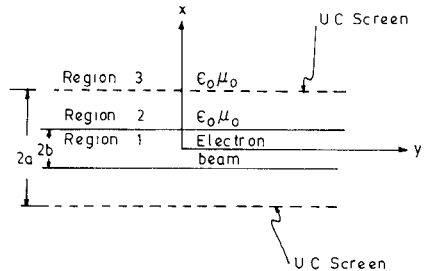


Fig. 2. Configuration considered for theoretical analysis. The structure is of infinite extent in  $y$ - and  $z$ -directions. The top and bottom UC screens conduct in directions making angles  $\theta$  and  $-\theta$ , respectively, with the  $y$ -axis.

For the transverse-symmetric modes, the longitudinal components in the different regions can be expressed in the form

$$E_z = \begin{cases} Ae^{-u(x-a)}, & x > a \\ B_1 e^{u(x-b)} + B_2 e^{-u(x-b)}, & b < x < a \\ C \sinh px, & x < b \end{cases} \quad (8)$$

$$H_z = \begin{cases} Me^{-u(x-a)}, & x > a \\ N \sinh ux, & x < a \end{cases} \quad (9)$$

where  $A, B_1, B_2$ , etc., are constant coefficients. These coefficients are related by the following boundary conditions:

- 1) Tangential components of electric and magnetic field are continuous at  $x = b$ ;
- 2) Tangential components of electric field are continuous at  $x = a$ ;
- 3) Electric field components are zero and the magnetic field components are continuous along  $y'$  at  $x = a$ .

The above boundary conditions result in the following characteristic equation for the transverse-symmetric modes:

$$(1 + \tanh ua) \tan^2 \theta = \frac{k_0^2}{u^2} \left[ 1 + \frac{\frac{p}{u} \coth pb + \tanh u(a-b)}{1 + \frac{p}{u} \coth pb \tanh u(a-b)} \right]. \quad (10)$$

For transverse-antisymmetric modes, the characteristic equation is

$$(1 + \coth ua) \tan^2 \theta = \frac{k_0^2}{u^2} \left[ 1 + \frac{\frac{p}{u} \tanh pb + \tanh u(a-b)}{1 + \frac{p}{u} \tanh pb \tanh u(a-b)} \right]. \quad (11)$$

Only the transverse-antisymmetric modes are of interest in the present context since only these modes have nonzero  $E_z$  along the axis. Solution of (10) and (11) gives the various possible modes propagating in the structure.

#### V. MODE VARIATION WITH DRIFT VELOCITY

As in the case of a helix-type of TWT [2], there is a strong interaction between the beam and the electromagnetic wave when the drift velocity of electrons is close to the phase velocity of the electromagnetic wave. In the presence of an electron beam, the normal mode of propagation in the structure breaks up into three independent forward modes. In Figs. 3 and 4, the real and imaginary parts of the propagation constant for the three modes are plotted as functions of beam voltage for two different sets of parameters. In order to facilitate comparison with the case of a circular helix, the parameters in Fig. 4 are chosen similar to those in [2]. When the difference between the phase velocity of

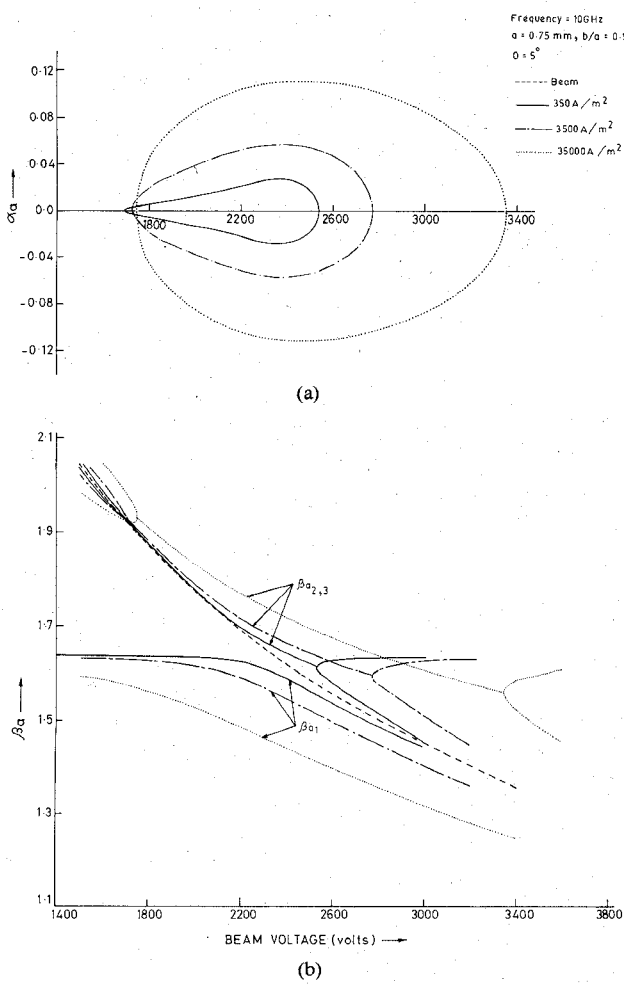


Fig. 3. (a) Attenuation constant and (b) phase constant versus beam voltage for  $b/a = 0.5$ ,  $a = 0.75 \text{ mm}$ , frequency = 10.0 GHz,  $\theta = 5^\circ$ , for three different values of beam density,  $J_0 = 350 \text{ A/m}^2$ ,  $J_0 = 3500 \text{ A/m}^2$ , and  $J_0 = 35000 \text{ A/m}^2$ .

the wave and the drift velocity of electrons is large, the three modes have no attenuation or amplification; the propagation constants are purely imaginary ( $\beta_1, \beta_2, \beta_3$ ). Over a finite range of electron velocity, when it is close to the phase velocity of the electromagnetic wave, two of the modes have complex propagation constants with the same value of imaginary parts but equal and opposite real parts. The mode with the negative attenuation constant increases as it advances along the structure, resulting in gain. With the increase of beam current, the velocity range over which amplification can occur increases and so does the maximum attainable amplification.

#### VI. NUMERICAL EXAMPLE FOR THE ORDER OF GAIN

Once the presence of the increasing mode in the planar TWT has been established, the order of magnitude of gain in a practical structure can be calculated. In general, there will be other modes also present at the input. In the present calculation, all these higher order modes are neglected and the input power is taken to be equally distributed in the three forward modes [8]. The gain of the planar TWT is given as

$$\text{gain} = -9.54 + 54.575 \left( \frac{\alpha a}{\beta_e a} \right) N \text{ dB}$$

where  $N$  is the length of tube in wavelengths. For a current density of  $31831 \text{ A/m}^2$ , the maximum attainable gain is 12 dB

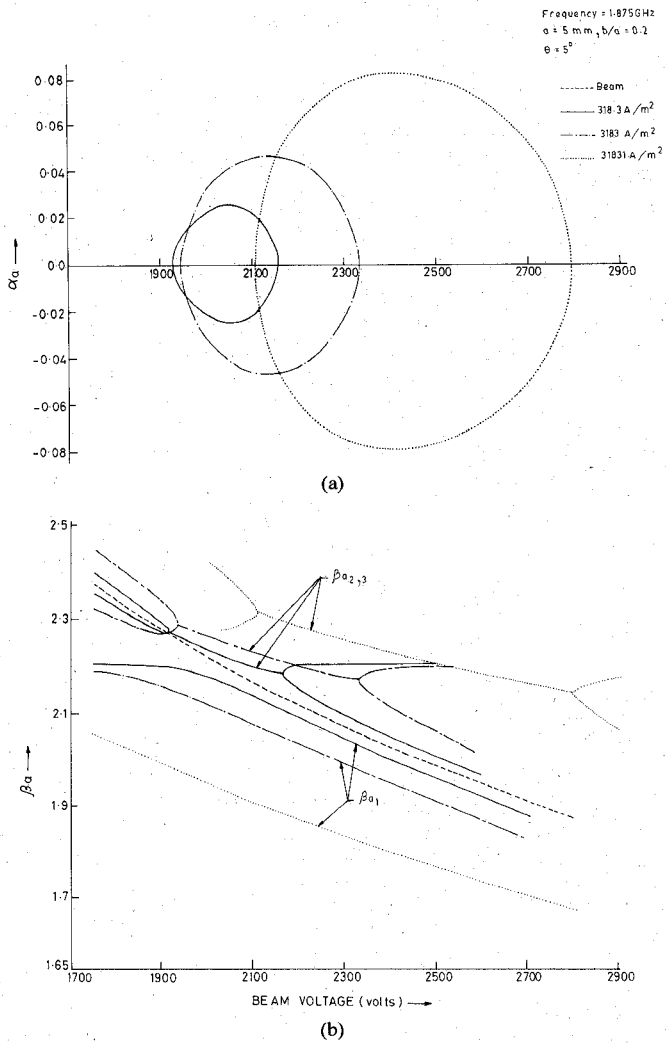


Fig. 4. (a) Attenuation constant and (b) phase constant versus beam voltage for  $b/a = 0.2$ ,  $a = 5 \text{ mm}$ , frequency = 1.875 GHz,  $\theta = 5^\circ$ , for three different values of beam density,  $J_0 = 318.3 \text{ A/m}^2$ ,  $J_0 = 3183 \text{ A/m}^2$ , and  $J_0 = 31831 \text{ A/m}^2$ .

for a structure ten wavelengths long, as derived from Fig. 4. It may be noted, for comparison, that the gain obtained in the case of a helix-type TWT for a corresponding set of parameters is 11.5 dB [2].

#### VII. CONCLUSIONS

An attempt has been made to show that a planar helix could be used as a slow-wave structure for TWT applications. The characteristics depicting the propagation constant as a function of beam voltage show that the structure is capable of providing amplification of the electromagnetic wave. The amplification compares well with the circular-helix TWT. The planar structure thus holds promise for application in TWT, with advantages of compatibility with microwave integrated circuits and ease of fabrication.

#### REFERENCES

- [1] J. R. Pierce, *Travelling-Wave Tube*. New York: Van Nostrand, 1950.
- [2] L. J. Chu and J. D. Jackson, "Field theory of traveling-wave tubes," *Proc. IRE*, vol. 36, pp. 853-863, July 1948.
- [3] R. Kompfner, "The traveling-wave-tube as amplifier at microwaves," *Proc. IRE*, vol. 35, pp. 124-128, Feb. 1947.
- [4] M. Chodorow and N. J. Nalos, "The design of high-power traveling-wave tubes," *Proc. IRE*, vol. 44, pp. 649-659, May 1956.
- [5] R. K. Arora, "Surface wave on a pair of parallel unidirectionally conduct-

ing screens," *IEEE Trans. Antennas Propagat.*, vol. AP-14, pp. 795-797, Nov. 1966

[6] S. Aditya, "Studies of a planar helical slow-wave structure," Ph.D. dissertation, Indian Institute of Technology Delhi, India, 1979

[7] S. Aditya and R. K. Arora, "Guided waves on a planar helix," *IEEE Trans. Microwave Theory Tech.*, vol. MTT-27, pp. 860-863, Oct. 1979

[8] R. E. Collin, *Foundations for Microwave Engineering*. New York: McGraw-Hill, 1966.

## Choosing Line Lengths for Calibrating Network Analyzers

CLETUS A. HOER, MEMBER, IEEE

**Abstract** — Equations, examples, and a table are given to help choose the best length for a precision transmission line which is used in some methods for calibrating a network analyzer. One line will cover a frequency range of about 10:1. Two lines will cover a range of about 65:1.

### I. INTRODUCTION

Some techniques for calibrating a network analyzer use a length of precision transmission line as the standard. Examples of such techniques are the "thru-reflect-line" technique [1] and the "thru-short-delay" technique [2]-[5]. One problem with using a length of line as the standard is that its electrical length must not be too near multiples of 180°, or the solution for the constants characterizing the network analyzer becomes ill-conditioned. An electrical length of 90° + 180°*m* is ideal, where *m* = 0, 1, 2, ... . Another problem is that the physical length of a line whose electrical length is less than 180° may be too short to be practical. Three methods of choosing the line lengths to avoid these problems are given in this short paper.

### II. SHORT LINES

Let the frequency range of the network analyzer be from *f*<sub>1</sub> to *f*<sub>2</sub>. If *f*<sub>2</sub>/*f*<sub>1</sub> is less than about 10, one line will frequently provide satisfactory performance over the whole operating range if its electrical length is 180° at the frequency *f*<sub>1</sub> + *f*<sub>2</sub>, as shown in Fig. 1. If the effective phase shift through the line is defined as the absolute difference between the actual phase shift and the closer of 0° or 180°, then the minimum effective phase shift through the line will be the same at both *f*<sub>1</sub> and *f*<sub>2</sub>, and the phase will be 90° at the center of the band.

The phase shift through an air-dielectric coaxial transmission line is [6]

$$\phi = 12fl \text{ deg} \quad (1)$$

where *f* is the frequency in gigahertz and *l* is the length in centimeters. For the phase shift to be 180° at *f*<sub>1</sub> + *f*<sub>2</sub>, the length of the coaxial line must be

$$l = \frac{15}{f_1 + f_2} \text{ cm,} \quad \text{for } f \text{ in gigahertz.} \quad (2)$$

Using (2) in (1), the phase shift at *f*<sub>1</sub> is

$$\phi_{f_1} = \frac{180}{1 + f_2/f_1} \text{ deg.} \quad (3)$$

Manuscript received April 30, 1982; revised August 23, 1982  
The author is with the National Bureau of Standards, Boulder, CO 80303

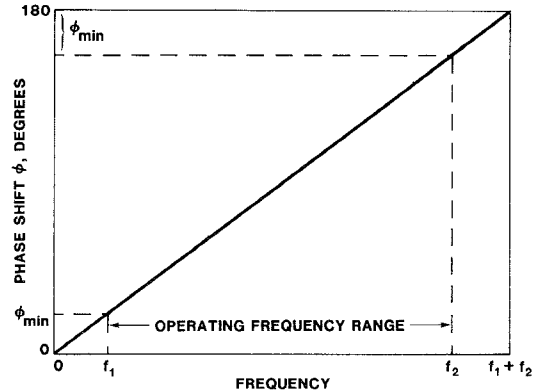


Fig. 1 Phase shift through a single transmission line designed to cover the frequency range *f*<sub>1</sub> to *f*<sub>2</sub>. The optimum length is that which gives a phase shift of 180° at *f*<sub>1</sub> + *f*<sub>2</sub>.

This is also the effective phase shift at *f*<sub>2</sub>. If the effective phase shift at *f*<sub>1</sub> and *f*<sub>2</sub> is too small, the frequency range *f*<sub>1</sub> to *f*<sub>2</sub> may be broken into two ranges, *f*<sub>1</sub> to *f*<sub>i</sub> and *f*<sub>i</sub> to *f*<sub>2</sub>, where *f*<sub>i</sub> is some intermediate frequency. A practical choice for *f*<sub>i</sub> is such that *f*<sub>2</sub>/*f*<sub>i</sub> = *f*<sub>i</sub>/*f*<sub>1</sub> =  $\sqrt{f_2/f_1}$ . If the line lengths for each range are chosen as described above, the phase angles at *f*<sub>1</sub>, *f*<sub>i</sub>, and *f*<sub>2</sub> calculated from (3) for the smaller ranges will then all be equal and as large as possible. This idea can obviously be extended to more than two ranges.

At the higher frequencies, the physical length *l* calculated from (2) may be too small to be practical. Then one must use either one or two longer lines as discussed below.

### III. ONE LONG LINE

As an alternative to the above, it is possible to use a longer line over an arbitrarily wide frequency range, although operation at certain bands of frequencies must be excluded to avoid associated phase shifts too near multiples of 180°. In this section is derived an expression for choosing equally spaced frequencies having phase angles which are a specified minimum distance from multiples of 180°.

Let the calibration frequencies be equally spaced a distance  $\Delta f$  apart. The corresponding changes in phase,  $\Delta\phi$ , from (1) will be

$$\Delta\phi = 12l\Delta f. \quad (4)$$

If the line length or the frequencies are chosen as shown in Fig. 2(a) so that the phase shifts nearest to 0° and 180° are a distance

$$\phi_{\min} = \frac{\Delta\phi}{2} \quad (5)$$

from 0° and 180°, then the effective phase shifts at all frequencies of measurement will be equal to or greater than  $\phi_{\min}$ . Adding the phase shifts from 0° to 180° in Fig. 2(a) gives

$$180^\circ = 2\phi_{\min} + n\Delta\phi, \quad n = 0, 1, 2, \dots \quad (6)$$

where *n* = 4 in Fig. 2(a). Eliminating  $\Delta\phi$  from (5) and (6) leads to

$$\phi_{\min} = \frac{90}{1+n}. \quad (7)$$

Thus  $\phi_{\min}$  is restricted to values of 90°, 45°, 22.5°, 18°, etc. Eliminating  $\Delta\phi$  from (4) and (5) gives

$$\Delta f = \frac{\phi_{\min}}{6l}. \quad (8)$$